# Phase field modeling of aluminum agglomeration in solid composite propellants

Matthew Mehrtens* and Brandon Runnels†
*Department of Aerospace Engineering, Iowa State University, Ames, IA, 50011*

**The agglomeration of aluminum (Al) nanopowder often causes efficiency losses during combustion and degradation of solid rocket motors during the burning of solid composite propellants (SCP). While physical experiments have provided valuable insights into Al agglomeration, the phenomenon is highly sensitive to propellant geometry and composition. As a result, numerical simulation provides a more versatile and systematic approach to exploring parameter spaces, particularly under conditions that are difficult, costly, or impractical to investigate experimentally. This work presents a computational model using phase field (PF) methods that simulates Al nanopowder agglomeration in an ammonium perchlorate/hydroxyl-terminated polybutadiene (AP/HTPB) SCP. The model is implemented in Alamo, an open-source, in-house multiphysics solver for PF simulations with block-structured adaptive mesh refinement (BSAMR). By running the model on a set of 100 packed-sphere microstructures with varying AP weight percentages (wt%) and particle sizes, the model's ability to capture the complex physics of agglomeration at the mesoscale is determined. Simulation results generally reflect the trends predicted by the pocket model, showing that Al agglomeration is more likely to occur in SCP formulations with lower AP loadings or with coarser AP particles.**

## I. Introduction

Solid rocket motors (SRM) that use solid composite propellants (SCP) have played a key role in improving the reliability and safety of rocket-powered launch and delivery systems. SRM performance is determined from factors ranging from grain geometry (which has been extensively studied) to SCP composition, which can be enhanced with burn rate modifiers or metal fuel additives. The use of additives results in a wide range of possible configurations and compositions, many of which have been experimentally explored. As manufacturing techniques advance and more SCP design space becomes accessible, there is a growing need for advanced simulation methods to predict SCP performance across arbitrary compositions, morphologies, and geometries.

Ammonium perchlorate/hydroxyl-terminated polybutadiene (AP/HTPB) propellants are a type of SCP commonly used in SRMs. To enhance performance, metal-based fuel additives are frequently introduced. Al nanopowder is commonly used because its geometry and chemical properties can increase the burn rate and decrease the pressure exponent [1]. However, adding Al nanopowder to AP/HTPB propellants can cause Al to accumulate and agglomerate at the burning surface during regression. This agglomeration can negatively impact regression by leading to incomplete combustion or even acoustic instabilities [2–4]. While these effects have been studied experimentally, there is still a lack of computational tools to model Al agglomeration and systematically quantify its impact on SCP performance.

The phase field (PF) method is well-suited for modeling Al agglomeration in the context of SCP burn. PF methods have been used successfully to capture regression rates, thermal evolution, burn surface morphology, and ignition behavior [5–7]. They have also been coupled directly to flow field simulations using the diffuse boundary method [8, 9]. Because they use implicit interfaces, PF methods can handle multiphysics problems in highly complex geometries. Since Al agglomeration is likely driven by a range of kinetic and dynamic mechanisms—including surface tension, burn rate, inertial effects, and elasticity—PF methods are particularly well-equipped to resolve these complexities. In this paper, we leverage the strengths of PF methods to couple and model Al agglomeration during AP/HTPB regression, with the goal of better understanding what parameters influence Al agglomeration.

*Graduate Research Assistant
†Associate Professor

## II. Phase Field Model

The simulation results presented in this work were generated using a novel PF method, the formulation of which is described here. The setting of this model is the thermally-informed phase field model originally developed and presented in Meier *et al* [7]; the reader is referred to that paper for details on the regression model.

### A. Order Parameters

The method presented in this work considers two phases (solid and gas) and three species (AP, HTPB, and Al). Both phase change and species variability are represented mathematically through the use of continually varying order parameters. Let $\Omega \subset \mathbb{R}^n$ be the domain of interest, and let $\eta \in C_2(\Omega, [0, 1])$ be an order parameter such that $\eta = 1$ represents unburned material (solid) and $\eta = 0$ represents burned material (gas). To model the different substances in the solid phase, we define two species parameters: the first, $\phi$, where $\phi = 1$ represents solid-phase AP and $\phi = 0$ represents solid-phase binder (that may or may not contain aluminum nanopowder). $\phi$ consequently has no significance when $\eta = 0$ To account for Al, an additional order parameter $\alpha \in C_2(\Omega, [0, 1])$ is used such that

$$\int_\Omega \alpha(\boldsymbol{x})\mathrm{dx} = \mathrm{V} \equiv \text{volume of agglomerate in } \Omega. \tag{1}$$

States in which aluminum mixes with AP in the solid phase at the sub-grid level are not considered. This is accounted for computationally through the prescription that if $\eta = 1$ and $\phi = 1$, then $\alpha$ is set to zero..

To determine the evolution of $\alpha$ it is first necessary to determine the thermodynamic free energy functional. First, the chemical potential of Al $W_C(\alpha)$ is defined such that the minimum energy states occur at $\alpha = 0$ and $\alpha = 1$:

$$W_C(\alpha) = \frac{\sigma}{\epsilon}\alpha^2(1-\alpha)^2, \tag{2}$$

where $\sigma$ is the interface energy and $\epsilon$ is the diffuse interface length parameter. Then, to capture the surface tension of the agglomerate, we define

$$W_B(\alpha) = \frac{1}{2}\sigma\epsilon|\nabla\alpha|^2. \tag{3}$$

Unlike with regression modeling, the surface tension in aluminum agglomeration is a key driving force due to the large effect of capillarity on aluminum droplet mgiration. Combining eqs. (2) and (3), the total portion of the free energy functional $F$ that depends on $\alpha$ is

$$F[\alpha] = \int_\Omega \left(W_C(\alpha) + W_B(\alpha)\right)\mathrm{dx} = \int_\Omega \left(\frac{\sigma}{\epsilon}\alpha^2(1-\alpha)^2 + \frac{1}{2}\sigma\epsilon|\nabla\alpha|^2\right)\mathrm{dx}.$$

To account for the mixing of Al and HTPB, the kinetic coeffficient ("mobility"), $L$, governing the evolution of $\alpha$, is defined as

$$L = L_0(1-\eta)^n, \tag{4}$$

where $\eta$ is the phase-change order parameter in the regression model, $L_0$ is the free-flow parameter, and $n > 0$ is a model constant. This definition guarantees that Al will not flow inside the binder (HTPB) but will move freely once $\eta = 0$.

With these definitions in hand, the kinetics of Al agglomeration are then modeled using Allen-Cahn kinetics (L2 gradient flow).

$$\frac{\partial\alpha}{\partial t} = -L\frac{\delta F}{\delta\alpha}. \tag{5}$$

Because Allen-Cahn is inherently non-conservative, the conservation of non-reacted Al must be enforced explicitly. Including this in the kinetic relation yields the final governing equation for $\alpha$,

$$\frac{\partial\alpha}{\partial t} = -L\left[\frac{\delta F}{\delta\alpha} + \lambda\left(\frac{V}{V_0} - 1\right)\right], \tag{6}$$

where $\lambda$ is a Lagrange multiplier that is suitably large to enforce the constraint up to tolerance, and $V_0$ is the initial volume of Al in the domain $\Omega$. This Lagrange multiplier drives the system to conserve the volume of Al in the domain, and can be interpreted as a constitutive resistance to compression (that is, a bulk modulus).

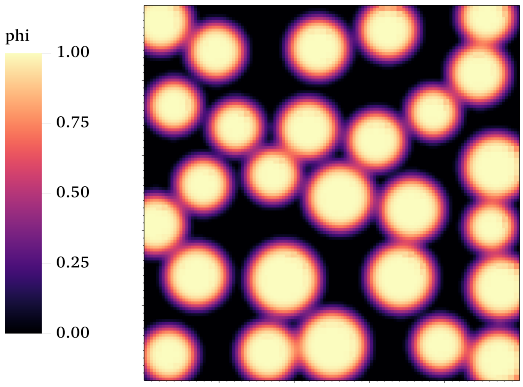


**(a) Species order parameter $\phi$ indicating oxidizer/binder.**

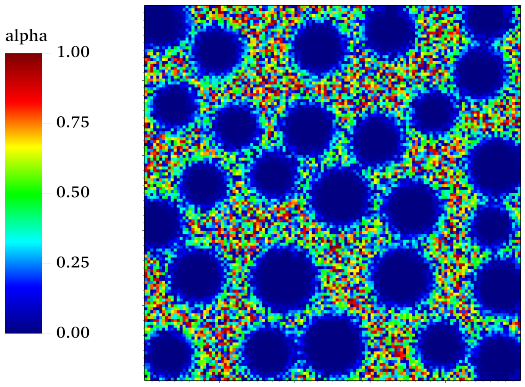


**(b) Aluminum order parameter $\alpha$ at initialization**

**Fig. 1 Initialization of species and aluminum order parameters in a representative example SCP geometry.**

## III. Numerical Implementation

The PF agglomeration model presented is implemented in Alamo, an in-house, open-source multiphysics solver for PF simulations built on AMReX, a block-structured adaptive meshing framework [10, 11]. The model is implemented on top of the existing combustion model [7] with one-way coupling from the combustion model to the agglomeration model. This architecture enables the agglomeration model to operate simultaneously alongside and be informed by a realistic propellant combustion simulation.

The microstructures considered in this work consist of non-overlapping circular AP particles in a square domain that is 500 µm × 500 µm (fig. 1a). The AP radii for each microstructure are randomly generated using a log-normal distribution and randomly placed in the domain. At initialization of the simulation and at each point in the domain, $\alpha$ is set by a random uniform distribution. Since $\alpha$ represents the volume fraction of Al (eq. (1)), individual particles of nanopowder Al are not resolved. It is noted that this random initial condition is not representative of optimized propellant formulations, where the vol% of Al would be more consistent throughout the binder. However, it adequately captures the effects of natural variations in nanopowder Al distribution throughout the propellant binder, which may be the impetus for the formation of agglomerates. After the $\alpha$ field has been initialized over the entire domain, it is multiplied by the complement of $\phi$ to ensure there is no Al in the crystalline AP phase (Fig. 1b).

It is noted that, beyond the explicit dependence on $\eta$ (eq. (4)) and the implicit dependence on $\phi$ in the initialization of the simulation, the model and its implementation featured in this work have minimal coupling between the existing combustion model and the agglomeration model. Furthermore, in the simulation results, the agglomerate phase does not influence the regression rate or combustion behavior. Although this is not physical (the coupling between agglomeration and regression is obviously bidirectional), it enables efficient implementation and rapid performance. Further coupling between the two models will enhance the model physicality and constitutes future work.

## IV. Results and Discussion

This section demonstrates the model's capabilities and presents the results from the AP distribution and sizing parameter study. It also aims to demonstrate how the model captures physical agglomeration behaviors and assess the extent to which the microstructure influences the agglomeration model. Additionally, the resulting trends are compared to those predicted by the pocket model (c.f. [12]).

Even with only basic coupling between the combustion model and the agglomeration model, several realistic agglomerate behaviors can be simulated with the proposed model (fig. 2). These behaviors include agglomerates nucleating where there is a high local density of nanopowder Al (fig. 2c), agglomerates being pulled along the regression surface by capillary forces (or similar) (fig. 2e), and agglomerates detaching from the regression surface (fig. 2f).

To determine the effect of AP volum percentage on agglomeration behavior, fifty SCP microstructures with circular AP particles were generated with a mean particle size of 35 µm while the AP vol% varied from 35% to 59% (fig. 3). Figures 3a and 3c demonstrate the agglomerate behavior for a relatively low packing of AP (38.5 vol% AP). Since the gaps between the AP particles are significant, the agglomerate does not detach and follows the burn surface to the edge of the domain (fig. 3c). The agglomerate is relatively large, owing to the large initial volume of Al in the

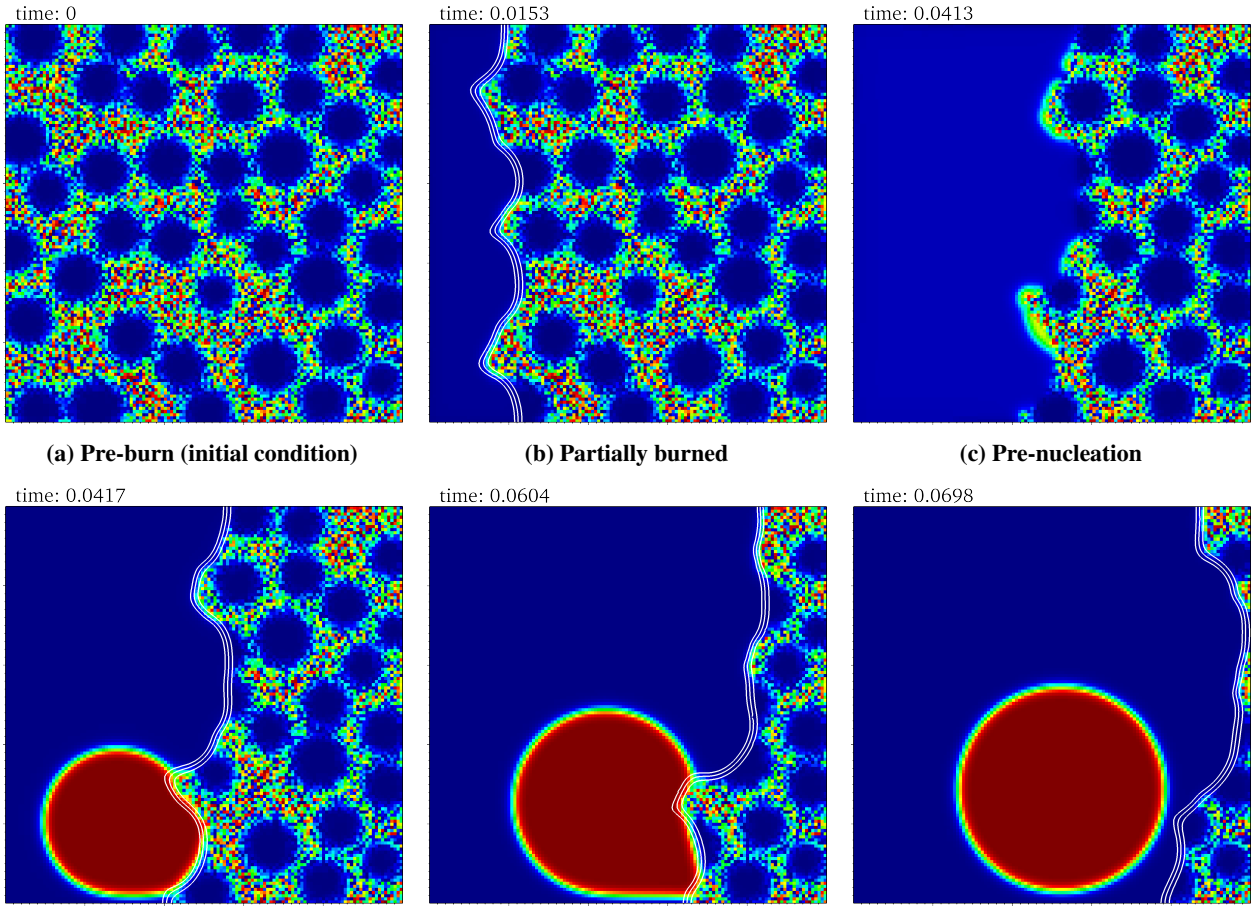


**(a) Pre-burn (initial condition)** **(b) Partially burned** **(c) Pre-nucleation**

**(d) Agglomerate nucleation** **(e) Capillary effects** **(f) Detachment**

**Fig. 2 Each stage of an agglomeration simulation using the model presented in this work. (a) The $\alpha$ (Al) phase is plotted; dark red represents $\alpha = 1$ (pure Al) and dark blue represents $\alpha = 0$ (no Al). The dark blue circles indicate circular AP particles. (b) The SCP has partially burned. The white contour lines denote a change in the solid phase order parameter $\eta$, *i.e.*, they represent the regression surface. (c) The state of the system just prior to nucleation of an agglomerate. Note the build-ups at the top and bottom of the regression surface that could grow to form the start of an agglomerate. (d) An agglomerate forms, quickly recovering the volume that had been lost from the domain. (e) The agglomerate is naturally pulled along the regression surface via capillary-like effects, caused by Eq. (3). (f) Due to the natural distribution of AP particles in the domain, the agglomerate detaches from the regression surface, and at this point, if a gas phase were coupled into the simulation, the agglomerate would likely move downstream into the flow.**

domain. Figures 3d and 3f show the agglomerate behavior (or lack thereof) for a higher packing of AP (58.5 vol% AP). Mid-burn, there are small hot spots where small agglomerates begin to form, but quickly dissipate (fig. 3e). Late in the burn, a pocket of Al in the top-right corner appears to be sufficiently large to spawn an agglomerate (fig. 3f). However, it does not ultimately agglomerate because the contribution of the Lagrangian volume constraint in Eq. (5) is too weak to overcome the activation energy required to nucleate an agglomerate.

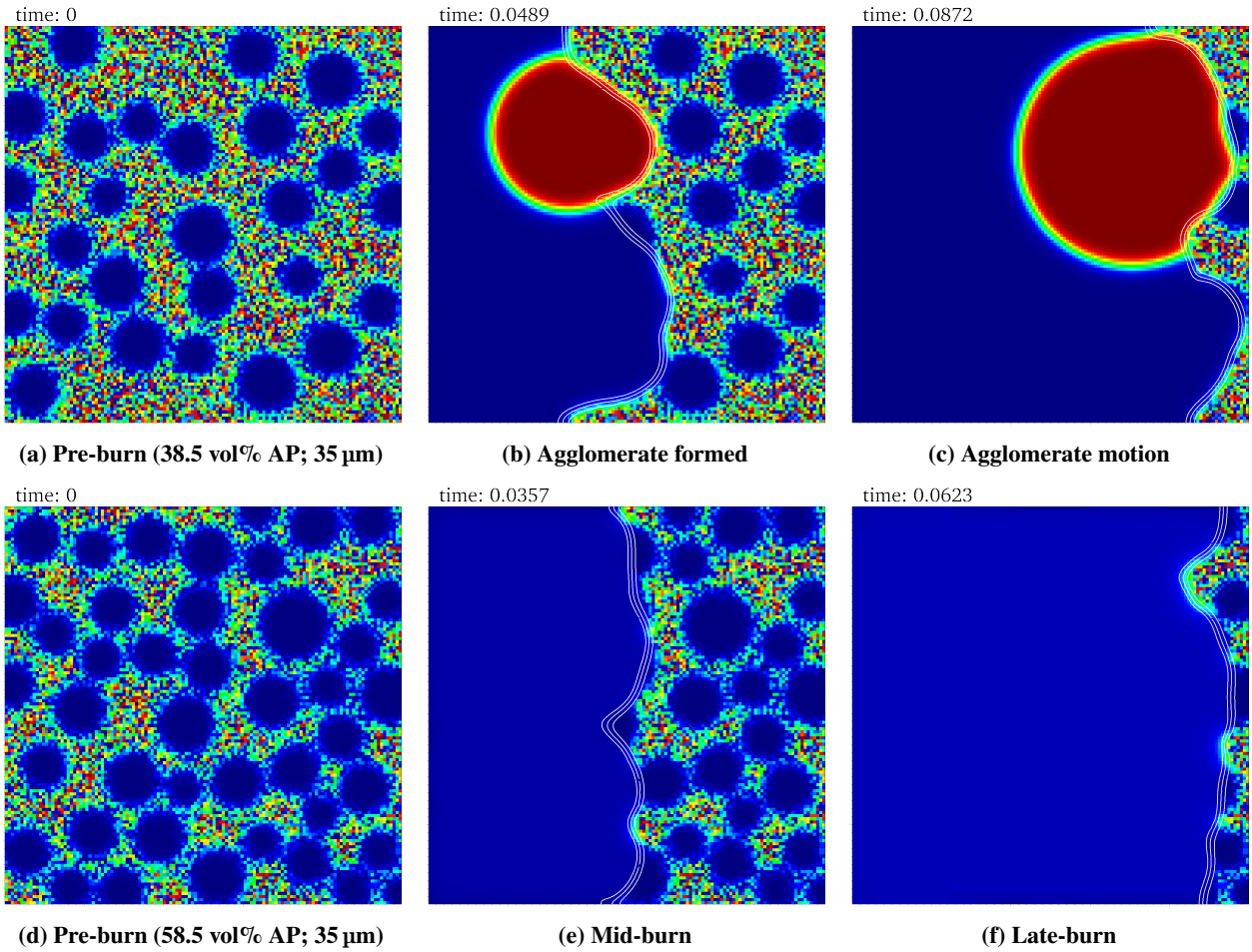


**(a) Pre-burn (38.5 vol% AP; 35 µm)** **(b) Agglomerate formed** **(c) Agglomerate motion**

**(d) Pre-burn (58.5 vol% AP; 35 µm)** **(e) Mid-burn** **(f) Late-burn**

**Fig. 3 Snapshots from two of the simulations in the first set of 50 microstructures where the mean AP particle size is held constant at 35 µm while the AP vol% is varied. In these figures, the $\alpha$ phase is plotted, and the regression surface is shown via the white contour lines. The top figures are from a configuration that produced an agglomerate, whereas the bottom figures are from a structure that did not produce an agglomerate.**

To determine the effect of AP particle size on agglomeration behavior, another 50 microstructures are considered that maintained an AP vol% of 50% while the mean AP particle size varied from 25 µm to 74 µm (fig. 4). Figures 4a and 4c show the conditions in which an agglomeration and detachment are likely to occur, even with coarse AP particles (54 µm mean radius). In the initial configuration, a clear pocket is visible between the coarse AP particles in the upper-right quadrant (fig. 4a). Because this is a large contiguous area of HTPB and Al, the agglomerate is likely to form in this pocket (Fig. 4b). After the agglomerate forms, it has no Al in the binder to attach to because of the encapsulating AP particles, and subsequently detaches from the regression surface (fig. 4c). Similar to the no agglomeration case shown in fig. 3, the fine AP particles in figs. 4d and 4f cause a reduction in pocket size between the AP particles, making a nucleation event less likely to occur. Figures 3e and 3f show there are small sites with a higher density of Al, but none sufficiently large to overcome the activation energy and nucleate an agglomerate (figs. 4e and 4f).

To identify general statistical agglomeration trends, each of the above cases is categorized as "forming an agglomerate" or "not forming an agglomerate" (fig. 5). As predicted by the pocket model [12], the chance of an agglomerate forming decreases as the AP loading increases or the AP mean particle size decreases. It is noted that even at the highest AP vol% in this study, it is still possible for an agglomerate to form (fig. 5a) due to the inherent stochasticity induced by the generation of microstructures. Despite the global configuration being unfavorable for agglomeration, if there are sufficiently high local densities of Al, the system may still produce an agglomerate. Similarly, despite having the same AP vol% for each simulation, when the mean AP particle size decreases sufficiently, it reduces the probability of a high local density of Al sufficient to produce an agglomerate (fig. 5b).

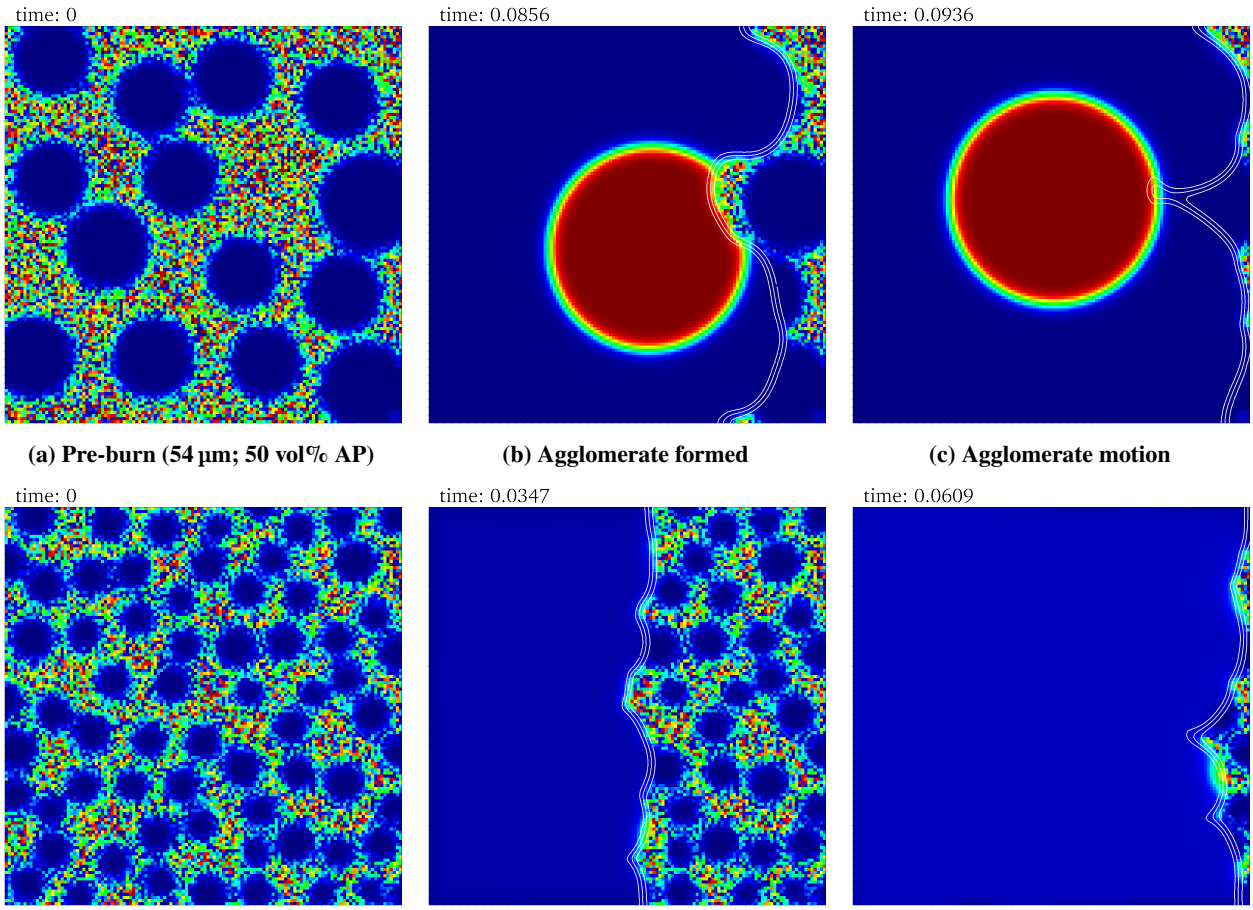


**(a) Pre-burn (54 µm; 50 vol% AP)** **(b) Agglomerate formed** **(c) Agglomerate motion**

**(d) Pre-burn (26 µm; 50 vol% AP)** **(e) Mid-burn** **(f) Late-burn**

**Fig. 4 Snapshots from two of the simulations in the second set of 50 microstructures where the AP vol% is held constant at 50 vol% AP while the mean AP particle size is varied. In these figures, the $\alpha$ phase is plotted, and the regression surface is shown via the white contour lines. The top figures are from a simulation that produced an agglomerate, whereas the bottom figures are from a configuration that did not produce an agglomerate.**

## V. Conclusions

Aluminized SCPs serve a vital role in national defense and space exploration. However, when embedded in the binder of an SCP, nanopowder Al tends to accumulate and agglomerate at the surface, causing efficiency losses and damage to the SRM. This work develops a novel PF model to simulate and computationally capture this agglomeration behavior. The model is integrated into Alamo, an in-house, open-source multiphysics solver for PF problems using BSAMR, and builds upon the existing combustion model by implementing a one-way coupling from the combustion model to the agglomeration model. The kinetics of the Al phase are driven by a volume-constrained Allen-Cahn equation.

The model was run on a series of HTPB/AP microstructures consisting of circular AP particles with varying properties to demonstrate the agglomeration model's ability to simulate realistic agglomeration behavior. It was shown that the model correctly captures trends predicted by the pocket model [12], *i.e.*, increasing the AP vol% or decreasing the mean AP particle size decreases the likelihood of agglomeration occurring.

Finally, a number of limitations of the work are acknowledged. First, as previously mentioned, this model considers only unidirectional coupling to the regression model, when in reality, the aluminum behavior would certainly affect the morphology of the burn surface to some degree. It is also noted that the current regression model does not resolve the gas phase, and so there is no interaction of the Al agglomerate with the gas phase. Therefore, the behavior of the agglomerate post-detachment does not account for viscous drag effects. Finally, this model presented in this section does not account for the reaction of Al, instead maintaining a constant total amount of Al during the course of the

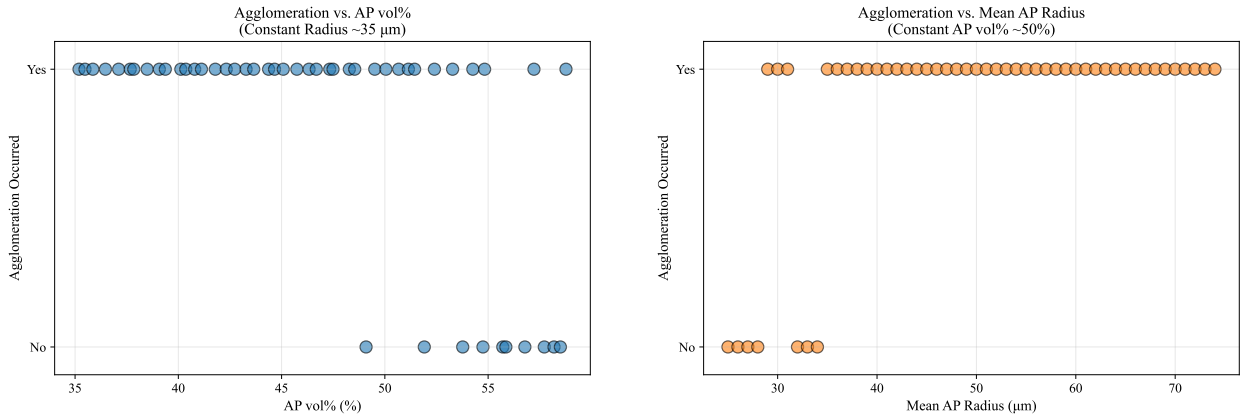


**(a) Whether the generated microstructure with a given AP vol% produced an agglomerate. In this dataset, the mean radius of the AP particles is maintained at 35 µm for each simulation.**

**(b) Whether the generated microstructure with a given mean AP particle radius produced an agglomerate. In this dataset, the AP vol% is maintained at 50% for each simulation.**

**Fig. 5 Results from the AP parameter study.**

simulation. While this is reasonable for ascertaining general agglomeration behaviors as affected by the mesostructure and regression behavior - which is the point of this work - additonal coupling is necessary before the simulation of post-agglomeration behavior is physically representative.

## VI. Acknowledgements

The acknowledge support from the Office of Naval Research, grant # N00014-25-1-2029. This work used the Nova cluster at Iowa State University.

## References

[1] Pang, W., Li, Y., DeLuca, L. T., Liang, D., Qin, Z., Liu, X., Xu, H., and Fan, X., "Effect of metal nanopowders on the performance of solid rocket propellants: A review," *Nanomaterials*, Vol. 11, No. 10, 2021, p. 2749.

[2] Gany, A., and Caveny, L. H., "Agglomeration and ignition mechanism of aluminum particles in solid propellants," *Symposium (International) on Combustion*, Vol. 17, Elsevier, 1979, pp. 1453–1461.

[3] Zhang, G., Liu, L., Wen, Z., Wang, Z., Liu, P., and Ao, W., "Experimental and numerical investigation of aluminum particle combustion driven instability in solid rocket motors," *Acta Astronautica*, Vol. 211, 2023, pp. 268–279.

[4] Han, L., Li, J., Wang, Y., Yu, W., Wang, J., Wang, N., and Wang, N., "Study on combustion oscillation characteristics of micron aluminum particles," *Powder Technology*, Vol. 394, 2021, pp. 782–790.

[5] Kanagarajan, B., Quinlan, J. M., and Runnels, B., "A diffuse interface method for solid-phase modeling of regression behavior in solid composite propellants," *Combustion and Flame*, Vol. 242, 2022, p. 112219.

[6] Kanagarajan, B., Quinlan, M., and Runnels, B., "Phase field modeling of solid phase AP/HTPB to determine the effect of particle distribution on regression rate," *AIAA SCITECH 2022 Forum*, 2022, p. 1899.

[7] Meier, M., Schmidt, E., Martinez, P., Quinlan, J. M., and Runnels, B., "Diffuse interface method for solid composite propellant ignition and regression," *Combustion and Flame*, Vol. 259, 2024, p. 113120.

[8] Schmidt, E. M., Quinlan, J. M., and Runnels, B., "Self-similar diffuse boundary method for phase boundary driven flow," *Physics of Fluids*, Vol. 34, No. 11, 2022.

[9] Schmidt, E. M., Quinlan, J. M., Bojko, B., and Runnels, B., "A Diffuse Interface Method for the Coupling of Solid and Gaseous Phases in a 1D Verification Problem for Combustion of AP/HTPB," *AIAA SCITECH 2022 Forum*, 2022, p. 2196.

[10] Runnels, B., Agrawal, V., and Meier, M., "The Alamo multiphysics solver for phase field simulations with strong-form mechanics and block structured adaptive mesh refinement," *arXiv preprint arXiv:2503.08917*, 2025.

[11] Zhang, W., Almgren, A., Beckner, V., Bell, J., Blaschke, J., Chan, C., Day, M., Friesen, B., Gott, K., Graves, D., et al., "AMReX: a framework for block-structured adaptive mesh refinement," *The Journal of Open Source Software*, Vol. 4, No. 37, 2019, p. 1370.

[12] Cohen, N. S., "A pocket model for aluminum agglomeration in composite propellants," *Aiaa Journal*, Vol. 21, No. 5, 1983, pp. 720–725.